# Comparison between different Gaussian series representations of the imaginary time propagator

Riccardo Conte* and Eli Pollak†
*Chemical Physics Department, Weizmann Institute of Science, 76100 Rehovoth, Israel*
(Received 20 December 2009; revised manuscript received 27 January 2010; published 18 March 2010)

A useful approximation for the thermal operator $\exp(-\beta\hat{H})$ is based on its representation in terms of either frozen or thawed Gaussian states. Such approximate representations are leading-order terms in respective series representations of the thermal operator. A numerical study of the convergence properties of the frozen Gaussian series representation has been recently published. In this paper, we extend the previous study to include also the convergence properties of the more expensive thawed Gaussian series representation of the thermal operator. We consider three different formulations for the series representation and apply them to a quartic double-well potential to find that the thawed Gaussian series representation converges faster than the frozen Gaussian one. Further analysis is presented as to the convergence properties and the numerical efficiency of three different thawed Gaussian series representation. The unsymmetrized form converges most rapidly, however, the lower order approximations of the symmetrized forms are more accurate. Comparison with a standard discretized path-integral evaluation demonstrates that the Gaussian based perturbation series representation converges much faster.

DOI: 10.1103/PhysRevE.81.036704 PACS number(s): 05.10.−a, 03.65.Sq, 05.30.−d, 02.70.Ss

## I. INTRODUCTION

The imaginary time propagator $\exp(-\beta\hat{H})$, where $\hat{H}$ is the Hamiltonian operator, lies at the heart of quantum thermodynamics. Many methods have been devised for its numerical computation in complex systems. Perhaps the most straightforward way is via path-integral Monte Carlo (PIMC) [1–3] which has been successfully applied to systems of hundreds of degrees of freedom. PIMC is though difficult to converge at low temperatures. It thus remains of interest to propose and study alternative and approximate methodologies. These include for example the use of effective variational potentials [4–7] or initial value representations (IVRs) which are based on Gaussian (coherent-state) wave packets.

The quantum-mechanical imaginary-time propagation of a wave function is governed by the Bloch equation:

$$-\frac{\partial}{\partial\tau}|\mathbf{q}_0,\tau\rangle = \hat{H}|\mathbf{q}_0,\tau\rangle, \tag{1.1}$$

where $\tau$ is the "imaginary time." (We will use Greek letters throughout to denote imaginary times.) The solution to Eq. (1.1) can be approximated by means of a Gaussian wave packet whose center (in configuration space) evolves in time, also known as a frozen Gaussian wave packet [8]. In addition one may allow the width to evolve in time and then one is considering a thawed Gaussian wave packet [9] whose generic coordinate representation is

$$\langle\mathbf{x}|G,\mathbf{q},\gamma\rangle = \exp\left\{-\frac{1}{2}[\mathbf{x}-\mathbf{q}(\tau)]^T G^{-1}(\tau)[\mathbf{x}-\mathbf{q}(\tau)]+\gamma(\tau)\right\}. \tag{1.2}$$

Here, $G(\tau)$ is a time-dependent width matrix with positive eigenvalues, the Gaussian center is $\mathbf{q}(\tau)$, and $\gamma(\tau)$ is a scale factor. Based on earlier work of Hellsing *et al.* [10], the thawed Gaussian approximation has been used extensively in recent years in a symmetrized form by Mandelshtam and Frantsuzov and co-workers [11–15], especially in the context of the thermodynamics of rare-gas clusters. However, Gaussian wave packets are not without problems, especially at low temperatures. Liu and Miller [16] noted that an approximation based only on Gaussian wave packets, whether frozen or thawed, cannot account for the correct structure of the Boltzmann operator in the low-temperature tunneling regime where typically the coordinate representation of the propagator has a double saddle-point structure. Therefore the Gaussian approximation for example cannot be used within the context of the quantum instanton approximation for reaction rates [17].

These deficiencies can be remedied at least in principle. In Ref. [18] it was pointed out that one can use the thawed Gaussian approximation in the context of a generalized time-dependent perturbation theory [19–21] to construct a series representation of the imaginary time propagator whose zeroth-order term is the symmetrized thawed Gaussian approximation.

Such a series representation was then implemented by Zhang *et al.* [22] employing the frozen Gaussian symmetrized approximation as the leading-order term in the series. The frozen Gaussian has the advantage that the time evolution, which is based on a modified dynamics, occurs only in configuration space. One must then solve $N$ coupled equations of motion when considering a system with $N$ degrees of freedom. In the thawed Gaussian form, the time dependence of the width matrix introduces an additional $N^2$ coupled equations of motion.

The purpose of this paper is to study the series representation of the imaginary time propagator, based on the thawed Gaussian zeroth-order solution. We also derive a new algorithm for the construction of the generalized time-dependent perturbation series. We then study three different ways to implement the series and compare the convergence proper-

*riccardo.conte@weizmann.ac.il
†eli.pollak@weizmann.ac.il

 

TABLE I. Number of configuration integrations $I(n)$ needed for the $n$th order in the thawed Gaussian series representation. Starting from fourth order, $I(n)$ of TEGA III is less than that of TEGA II.

| $n$ | TEGA I | TEGA II | TEGA III |
|---|---|---|---|
| 0 | 0 | 1 | 1 |
| 1 | 1 | 2 | 3 |
| 2 | 2 | 4 | 4 |
| 3 | 3 | 5 | 5 |
| **4** | **4** | **7** | **6** |

ties with those found when using the frozen Gaussian based series representation. We also present a comparison between the convergence of the Gaussian series based representation and a discretized path-integral evaluation.

The generalized perturbation theory and its three variants for the thawed Gaussian representation are presented in Sec. II. Numerical examples, the comparison with the frozen Gaussian and standard path-integral estimates are provided in Sec. III. We find that the thawed Gaussian series representations converge more rapidly than the frozen Gaussian and that the Gaussian series representation is much more efficient than the standard path-integral estimate especially at low temperature. We end with a Discussion of the relative efficacy of using the different methods at low temperature.

## II. SERIES REPRESENTATIONS FOR THAWED GAUSSIANS

The basic thawed Gaussian approximation $\hat{K}_0(\tau)$ for the exact imaginary time propagator $\hat{K}(\tau)=\exp(-\hat{H}\tau)$, which we will refer to as the time-evolved Gaussian approximation (TEGA I) is

$$\langle \mathbf{x}|\hat{K}_0(\tau)|\mathbf{q}_0\rangle = \left(\frac{1}{2\pi}\right)^{N/2}\frac{1}{\det[G(\tau)]^{1/2}}\exp\left\{-\frac{1}{2}[\mathbf{x}-\mathbf{q}(\tau)]^T \times G(\tau)^{-1}[\mathbf{x}-\mathbf{q}(\tau)]+\gamma(\tau)\right\}. \tag{2.1}$$

The time dependence of the Gaussian center, Gaussian width matrix and scale factor is determined by the following evolution equations [10–12]:

$$\frac{d}{d\tau}\mathbf{q}(\tau) = -G(\tau)\langle \nabla V(\mathbf{q}(\tau))\rangle, \tag{2.2}$$

$$\frac{d}{d\tau}G(\tau) = -G(\tau)\langle \nabla\nabla^T V(\mathbf{q}(\tau))\rangle G(\tau) + \hbar^2 I, \tag{2.3}$$

$$\frac{d}{d\tau}\gamma(\tau) = -\frac{1}{4}\mathrm{Tr}[\langle \nabla\nabla^T V(\mathbf{q}(\tau))\rangle G(\tau)] - \langle V(\mathbf{q}(\tau))\rangle. \tag{2.4}$$

The boundary conditions for each of these equations are

$$\mathbf{q}(\tau\approx 0)=\mathbf{q}_0, \quad G(\tau\approx 0)=\hbar^2\tau I, \quad \gamma(\tau\approx 0)=-\tau V(\mathbf{q}_0). \tag{2.5}$$

The brackets in Eqs. (2.2)–(2.4) denote the Gaussian average:

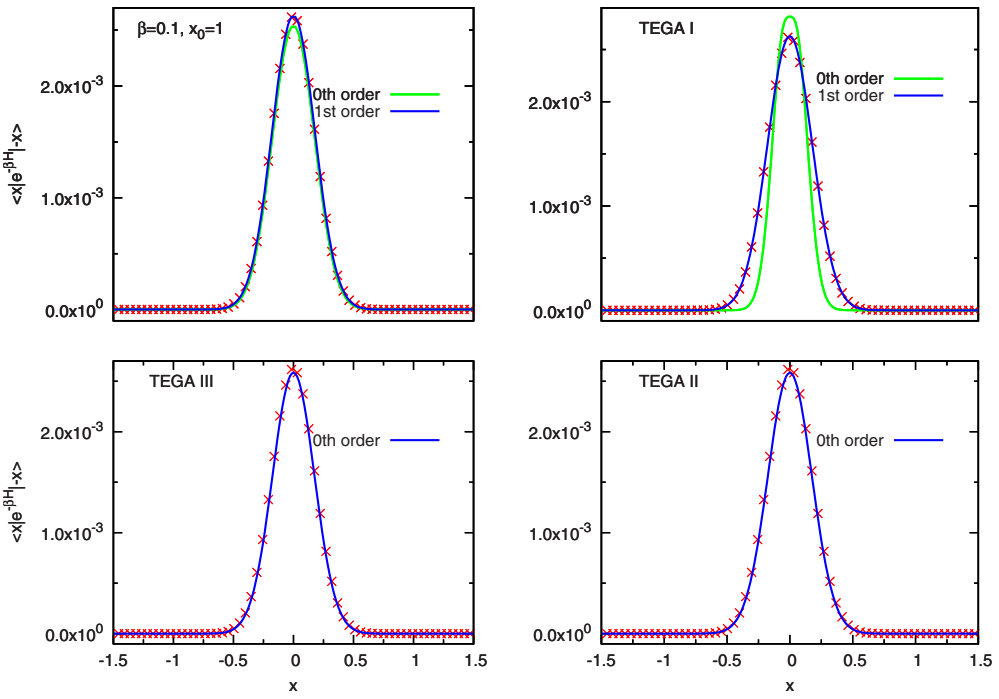


FIG. 1. (Color online) Convergence of different Gaussian series for the antisymmetric matrix element of the thermal operator at high temperature ($\beta$=0.1). The crosses represent the exact quantum-mechanical solution obtained by direct diagonalization of the Hamiltonian. The optimized frozen Gaussian results are given in the top left panel; TEGA I, II, and III follow clockwise.

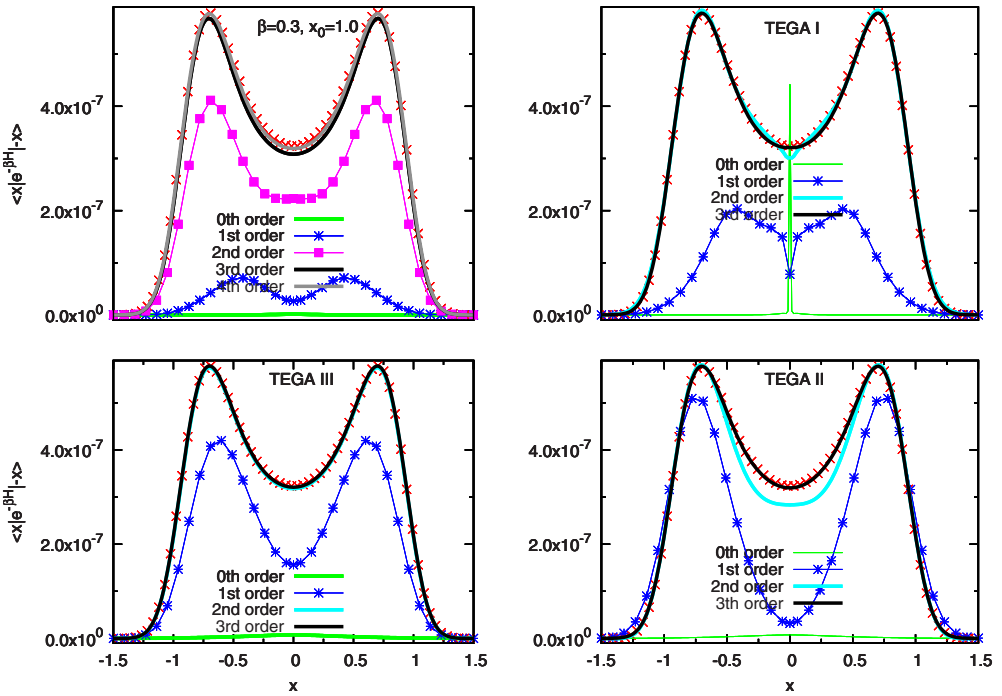


FIG. 2. (Color online) Convergence of different Gaussian series for the antisymmetric matrix element of the thermal operator around the crossover temperature ($\beta$=0.3). The notation is as in Fig. 1.

$$\langle f(\mathbf{q})\rangle = \left(\frac{1}{\pi}\right)^{N/2} \frac{1}{\det[G(\tau)]^{1/2}} \int d\mathbf{x} \times \exp\{-[\mathbf{x}-\mathbf{q}(\tau)]^T G(\tau)^{-1}[\mathbf{x}-\mathbf{q}(\tau)]\} f(\mathbf{x}). \tag{2.6}$$

We note that for the thawed Gaussian methodology the initial value of the width matrix is dictated by the condition that initially ($\tau$=0) the approximate propagator reduces to the identity operator. This differs from the frozen Gaussian approximation, where one has freedom in choosing the value of the constant width parameter. It was shown in Ref. [22] that the accuracy of the frozen Gaussian approximation depends sensitively on the choice of the width parameter. One optimizes it by minimizing the first-order correction to the partition function, relative to the zeroth-order term.

The propagator $\hat{K}_0$ is an approximation to the exact propagator $\hat{K}$. One can then associate with it a "correction operator" which provides a measure of how far the approximate operator is from the exact one. It is defined as

$$\hat{C}(\tau) = \left(-\frac{\partial}{\partial\tau} - \hat{H}\right)\hat{K}_0(\tau). \tag{2.7}$$

The formal solution of this equation is readily found to be

$$\hat{K}_0(\tau) = \hat{K}(\tau) - \int_0^\tau d\tau_1 \hat{K}(\tau-\tau_1)\hat{C}(\tau_1). \tag{2.8}$$

One may then expand the exact propagator as a power series in the correction operator:

$$\hat{K}(\tau) = \sum_{j=0}^{\infty} \hat{K}_j(\tau), \tag{2.9}$$

where we assume that $\hat{K}_j \sim \hat{C}^j$. Inserting this into the formal solution given in Eq. (2.8) leads to the recursion relation:

$$\hat{K}_{j+1}(\tau) = \int_0^\tau d\tau' \hat{K}_j(\tau-\tau')\hat{C}(\tau'), \quad j \geq 0. \tag{2.10}$$

The expression for the correction operator has been worked out in Ref. [18], one finds

$$\langle \mathbf{x}|\hat{C}(\tau)|\mathbf{q}_0\rangle = -\langle V_1(\mathbf{x},\mathbf{q},\tau)\rangle\langle \mathbf{x}|\hat{K}_0(\tau)|\mathbf{q}_0\rangle, \tag{2.11}$$

where the "potential nonlinearity term" $\langle V_1(\mathbf{x},\mathbf{q},\tau)\rangle$ contains all the derivatives of the potential which are higher than second order. Equations (2.1)–(2.11) represent a first practical generalized perturbation theory route for calculation of the exact quantum thermal operator.

A second way (TEGA II) of calculating the thermal operator stems from the fact that it is Hermitian:

$$\langle \mathbf{x}|\hat{K}(\tau)|\mathbf{x}'\rangle = \langle \mathbf{x}|\hat{K}(\tau/2)\hat{K}^\dagger(\tau/2)|\mathbf{x}'\rangle = \int d\mathbf{y}\langle \mathbf{x}|\hat{K}(\tau/2)|\mathbf{y}\rangle\langle \mathbf{y}|\hat{K}^\dagger(\tau/2)|\mathbf{x}'\rangle. \tag{2.12}$$

By insertion of Eq. (2.9) into Eq. (2.12), one readily finds

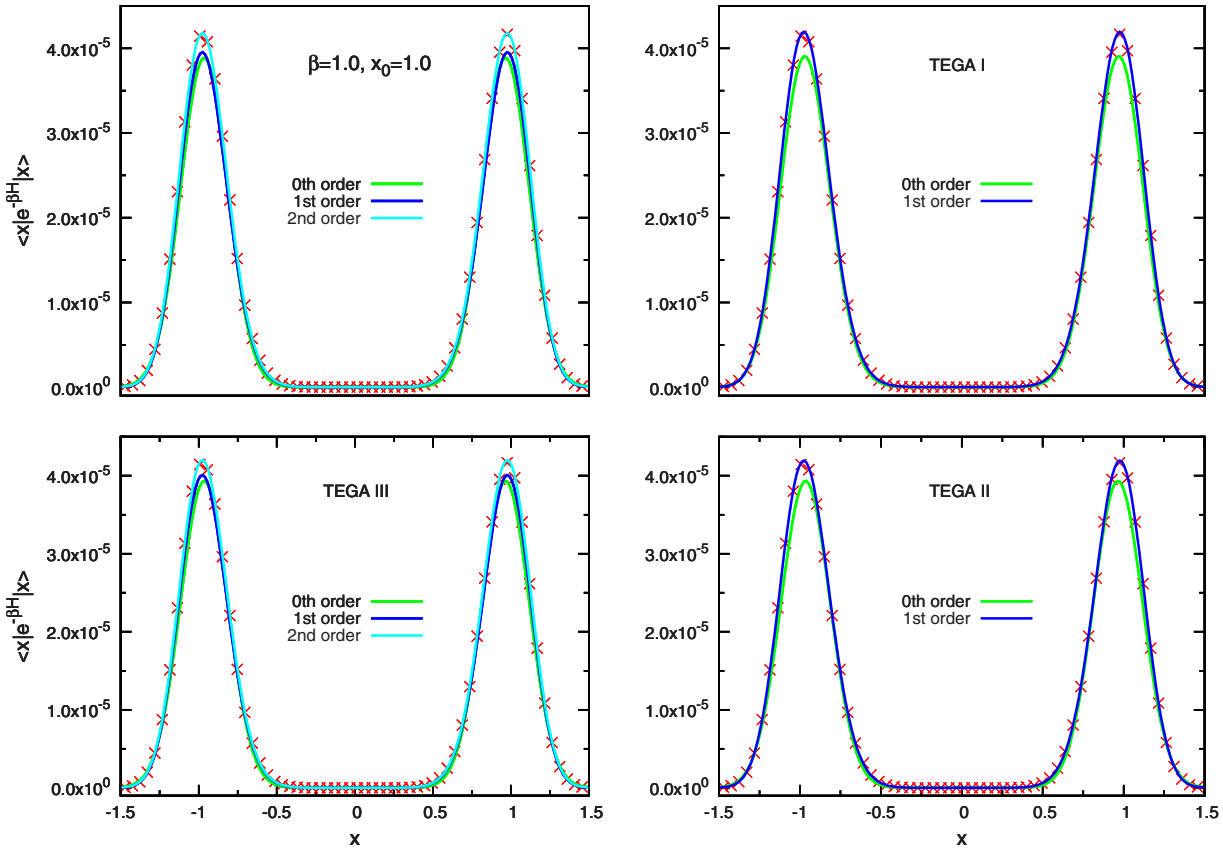


FIG. 3. (Color online) Convergence of different Gaussian series for the diagonal matrix element of the thermal operator at low temperature ($\beta$=1.0). The notation is as in Fig. 1.

$$\langle \mathbf{x}|\hat{K}(\tau)|\mathbf{x}'\rangle = \sum_{i,j=0}^{\infty} \int d\mathbf{y}\langle \mathbf{x}|\hat{K}_i(\tau/2)|\mathbf{y}\rangle\langle \mathbf{y}|\hat{K}_j^{\dagger}(\tau/2)|\mathbf{x}'\rangle. \tag{2.13}$$

Assuring this symmetry already for the zeroth-order term was one of the important contributions of the methodology used in Refs. [11,12]. This leading-order term

$$\begin{aligned}\langle \mathbf{x}|\hat{K}_0^s(\tau)|\mathbf{x}'\rangle = \int d\mathbf{q}\left(\frac{1}{2\pi}\right)^N \frac{\exp[2\gamma(\tau/2)]}{\det[G(\tau/2)]} \\ \times \exp\left\{-\frac{1}{2}[\mathbf{x}-\mathbf{q}(\tau/2)]^T G(\tau/2)^{-1} \right. \\ \left. \times[\mathbf{x}-\mathbf{q}(\tau/2)]\right\} \\ \times \exp\left\{-\frac{1}{2}[\mathbf{x}'-\mathbf{q}(\tau/2)]^T G(\tau/2)^{-1} \right. \\ \left. \times[\mathbf{x}'-\mathbf{q}(\tau/2)]\right\},\end{aligned} \tag{2.14}$$

like the exact propagator is symmetric. It requires to evolve the dynamics [Eqs. (2.2)–(2.4)] only up to $\tau/2$ at the cost of an additional integration over the configuration space, as compared with TEGA I. This then implies that higher-order terms are much more "expensive." Consider for example the first-order correction, it involves the multiplication of three propagators and thus two coordinate integrations. TEGA I involves a product of only two operators and thus one coordinate integration. On the other hand, due to the symmetry which is included term by term, one might expect that this second approach will converge faster than the first approach. The price to pay is the additional integration, and the increasing number of terms that contribute to each order in the perturbation series. This makes it computationally more expensive especially for high-dimensional systems.

A third series representation (TEGA III) is obtained by application of Eq. (2.7) directly to Eq. (2.14). The correction operator is then

$$\begin{aligned}\langle \mathbf{x}|\hat{C}_0^s(\tau)|\mathbf{x}'\rangle = \int d\mathbf{q}\Delta V(\mathbf{x},\mathbf{x}',\mathbf{q};\tau/2)\left(\frac{1}{2\pi}\right)^N \frac{\exp[2\gamma(\tau/2)]}{\det[G(\tau/2)]} \\ \times \exp\left\{-\frac{1}{2}[\mathbf{x}-\mathbf{q}(\tau/2)]^T \right. \\ \left. \times G(\tau/2)^{-1}[\mathbf{x}-\mathbf{q}(\tau/2)]\right\} \\ \times \exp\left\{-\frac{1}{2}[\mathbf{x}'-\mathbf{q}(\tau/2)]^T G(\tau/2)^{-1} \right. \\ \left. \times[\mathbf{x}'-\mathbf{q}(\tau/2)]\right\},\end{aligned} \tag{2.15}$$

where the potential nonlinearity term is

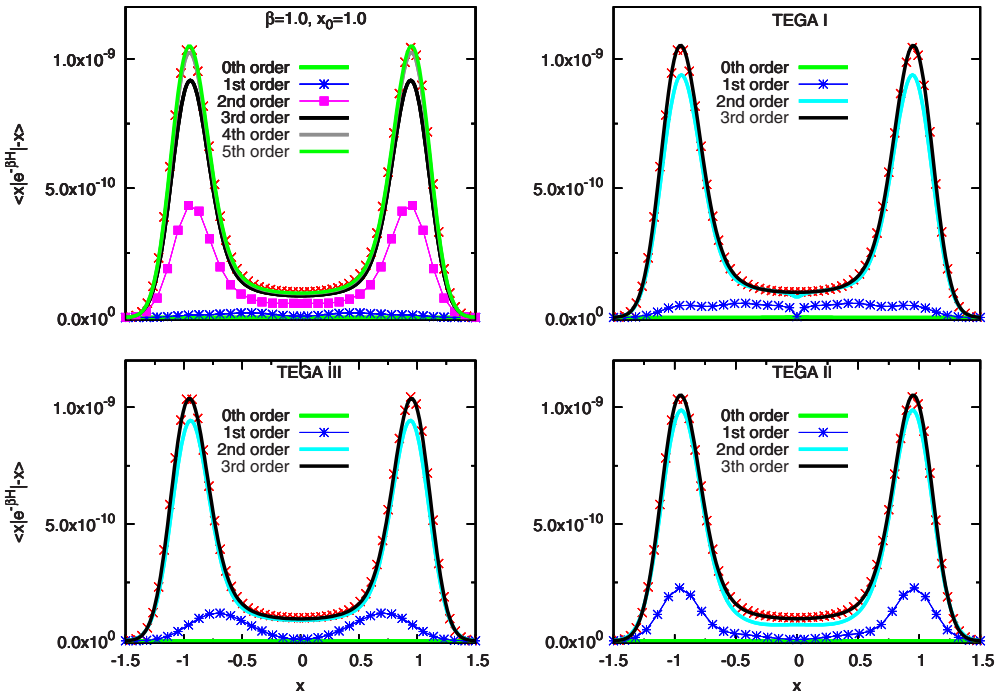


FIG. 4. (Color online) Convergence of different Gaussian series for the antisymmetric matrix element of the thermal operator at low temperature ($\beta=1.0$). The notation is as in Fig. 1.

$$\Delta V(\mathbf{x},\mathbf{x}',\mathbf{q};\tau/2) = -\frac{d\gamma(\tau/2)}{d\tau} + \frac{d\ln[\det G(\tau/2)]}{d\tau}$$
$$-\frac{1}{4}\frac{d\mathbf{q}^T(\tau/2)}{d\tau}G(\tau/2)^{-1}\{[\mathbf{x}-\mathbf{q}(\tau/2)]$$
$$+[\mathbf{x}'-\mathbf{q}(\tau/2)]\} - \frac{1}{4}\{[\mathbf{x}-\mathbf{q}(\tau/2)]^T$$
$$+[\mathbf{x}'-\mathbf{q}(\tau/2)]^T\}G(\tau/2)^{-1}\frac{d\mathbf{q}(\tau/2)}{d\tau}$$
$$+\frac{1}{2}[\mathbf{x}-\mathbf{q}(\tau/2)]^T\frac{d}{d\tau}G(\tau/2)^{-1}[\mathbf{x}-\mathbf{q}(\tau/2)]$$
$$+\frac{1}{2}[\mathbf{x}'-\mathbf{q}(\tau/2)]^T\frac{d}{d\tau}G(\tau/2)^{-1}[\mathbf{x}'-\mathbf{q}(\tau/2)]$$
$$+\frac{\hbar^2}{2}[\mathbf{x}-\mathbf{q}(\tau/2)]^T G(\tau/2)^{-1}G(\tau/2)^{-1}$$
$$\times[\mathbf{x}-\mathbf{q}(\tau/2)] - \frac{\hbar^2}{2}\mathrm{Tr}[G(\tau/2)^{-1}] - V(x). \tag{2.16}$$

TEGA III may be considered as a compromise route between TEGA I and TEGA II. It retains the symmetry of the zeroth-order term, however, just as in TEGA I, successive terms in the perturbation series are not symmetric. Since the zeroth-order term involves a coordinate integration, one finds that the first-order term needs three coordinate integrations, one more than TEGA II. However, the number of terms that contribute to each order is less, and stepping up to the next order requires only one additional integration for TEGA III so that for the fourth-order correction and higher it becomes less expensive than TEGA II.

More generally, for the $n$th-order propagator, the number of configuration integrations needed by the different approaches is given by the function

$$I(n) = \begin{cases} n & \text{TEGA I} \\ \frac{3n}{2}+1 & \text{if } n \text{ even} \\ & \text{TEGA II} \\ \frac{3n}{2}+\frac{1}{2} & \text{if } n \text{ odd} \\ 1 & \text{if } n=0 \\ & \text{TEGA III.} \\ n+2 & \text{if } n>0 \end{cases} \tag{2.17}$$

Table I presents the values of $I(n)$ up to fourth order.

## III. APPLICATION TO A QUARTIC DOUBLE-WELL POTENTIAL

We apply the three methods to the case of a quartic double-well potential

$$V(x) = -\frac{\omega^2}{2}x^2\left(1-\frac{x^2}{2x_0^2}\right) + \frac{\omega^2 x_0^2}{4} \tag{2.18}$$

employing the parameter values used in Ref. [22]: $\hbar=1$; $\omega=16$ (the frequency of the barrier); the minima of the potential are at the anharmonicity length $x_0=1$.

The Gaussian averaged potential is

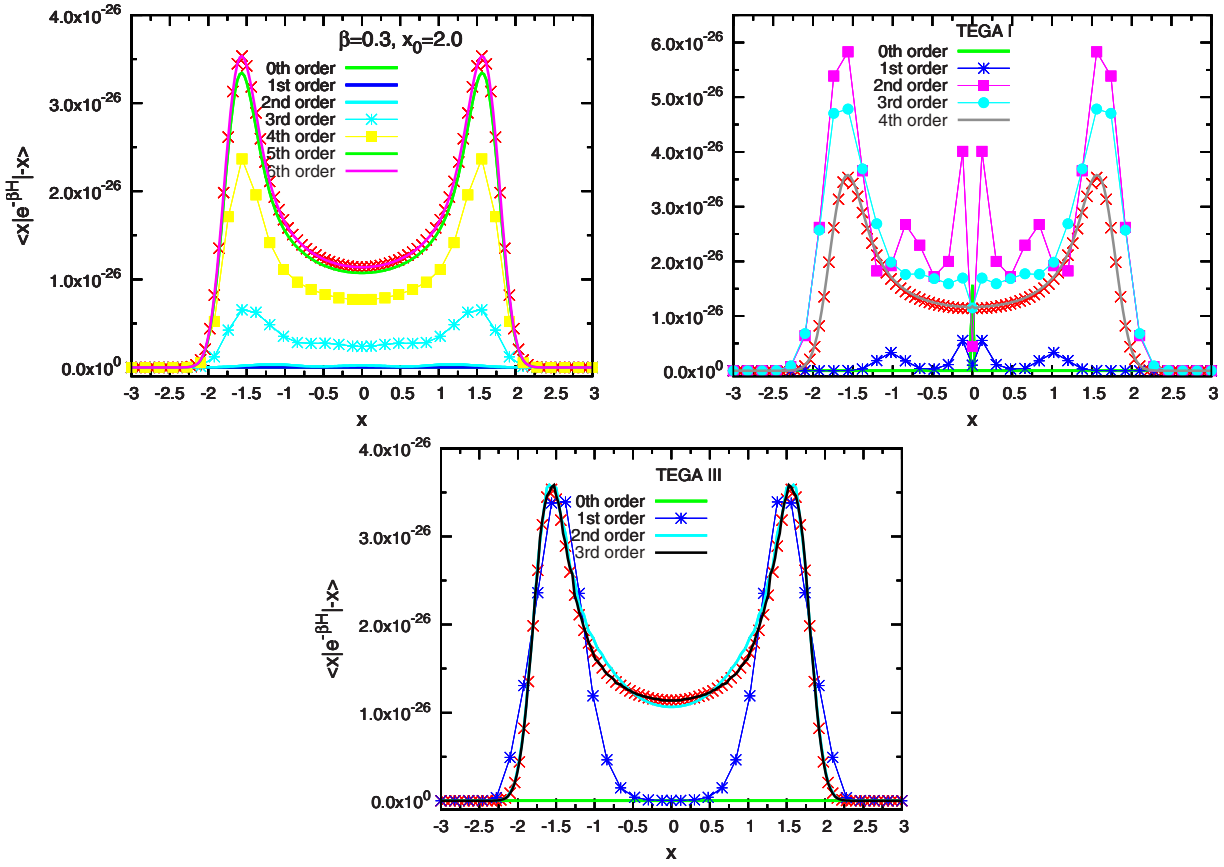


FIG. 5. (Color online) Convergence of different Gaussian series for the antisymmetric matrix element of the thermal operator at moderate temperature ($\beta$=0.3) but with a well that supports approximately 12 bound states ($x_0$=2). The notation is as in Fig. 1.

$$\langle V(q)\rangle = V(q) + \frac{3G\omega^2 q^2}{4x_0^2} - \frac{\omega^2 G}{4} + \frac{3G^2\omega^2}{16x_0^2} \qquad (2.19)$$

so that $\langle \nabla V(q)\rangle$ and $\langle \nabla\nabla^T V(q)\rangle$ are readily found by derivation.

Calculations were performed by means of grid representations for the zeroth-order propagators and the corresponding correction operators. Higher-order terms in the series were obtained by matrix multiplication and numerical time integration. Results are presented for diagonal $\langle x|\exp(-\beta\hat{H})|x\rangle$ and antisymmetric $\langle x|\exp(-\beta\hat{H})|-x\rangle$ matrix elements as a function of the coordinate, employing the three different TEGA methods and comparing them with the frozen Gaussian based results of Ref. [22]. The diagonal element is related to the classical localization of the wave function in the region of the wells, while the antisymmetric element depends sensitively on tunneling through the barrier. One thus expects the perturbation series to converge much faster for the diagonal element. The crossover temperature, defined as $\hbar\beta\omega=2\pi$, separates between the activation and tunneling regimes [23].

In Fig. 1 we present results for temperatures ($\hbar\beta\omega$=1.6) significantly above the crossover temperature. The zeroth-order diagonal element is almost perfect for all four methods under study and so there is no need to plot it. Differences do show up even at this high temperature when considering the antisymmetric matrix element. As may be seen from the figure, the zeroth-order term in the perturbation series is already accurate for the TEGA II and TEGA III methods (the leading-order term for these two methods is the same). The optimized frozen Gaussian result is slightly worse than TEGA II while TEGA I seemingly gives the worst result. However, one should note that the numerical effort of first-order TEGA I is comparable to the numerical effort needed for zeroth-order TEGA II since the former and the latter need one coordinate integration only (see Table I).

Results for a temperature ($\hbar\beta\omega$=4.8) which is only slightly above the crossover temperature are shown in Fig. 2. Also at this temperature, the leading diagonal term in the series is accurate for all four methods under consideration. We therefore provide results only for the antisymmetric matrix element. Here the differences between the various methods are larger. It is evident that the frozen Gaussian is the worst, one needs to go to fourth order in the perturbation series to converge to the exact result. TEGA III does best, it is essentially converged already with second-order perturbation theory, while TEGA I and TEGA II are of comparable accuracy, one must go to third order to converge to the numerically exact answer. Here too though one must consider the number of coordinate integrations needed to converge. As seen from Table I third-order TEGA I implies altogether six configuration integrations and six time integrations. Second-order TEGA III involves eight configuration integrations and three time integrations while third-order TEGA II

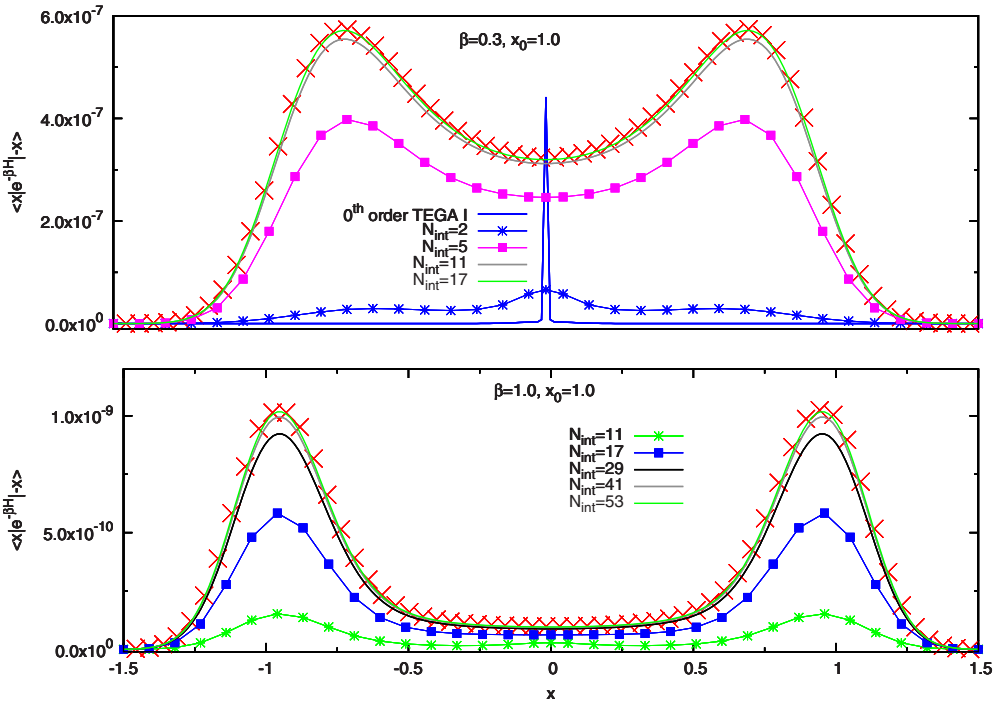


FIG. 6. (Color online) Convergence of a discretized path-integral representation for the antisymmetric matrix element of the thermal operator at moderate (top panel, $\beta=0.3$) and low (bottom panel, $\beta=1$) temperature with a well that supports approximately 6 bound states ($x_0=1$). The numerically exact results are denoted by the crosses. $N_{int}$ represents the number of time slices used.

involves 12 coordinate integrations and six time integrations. It would thus seem that in this case, the unsymmetrized series given by TEGA I is the most efficient.

The deep tunneling regime ($\hbar\beta\omega=16$) is studied in Figs. 3 and 4. Even at this low temperature, all methods do rather well for the diagonal matrix element as shown in Fig. 3. One may group the methods into pairs. TEGA III and the frozen Gaussian method need second-order perturbation theory to converge while TEGA I and TEGA II converge already with first order. Again though, the numerical effort involved in TEGA I is smaller than that of TEGA II. More noticeable differences emerge when considering the antisymmetric matrix element, as shown in Fig. 4. The frozen Gaussian method converges only at the fifth order while all TEGA methods converge already at the third order. Clearly, the thawed Gaussian methods are more accurate as one goes deeper into the tunneling regime. Again, the TEGA I method is the "cheapest" relative to TEGA II and III. Although all three methods must go to third order, the number of configuration integrations needed for TEGA I (6) is significantly smaller than the number needed for TEGA II (12) or TEGA III (13). We do note though that the zeroth and first-order results of TEGA I are qualitatively wrong. The differences between TEGA II and TEGA III are small, both converge to the exact answer by the third order, and in both cases the second-order result is already rather good.

We also studied the tunneling matrix element for a quartic double-well potential with a larger barrier, using $x_0=2$. The results for the antisymmetric matrix element and for temperature $\hbar\beta\omega=4.8$ are shown in Fig. 5. These results were obtained by using quartic precision arithmetic, needed for the very small magnitude of the matrix elements. As in the previous cases, the thawed Gaussian series converges much more rapidly than the frozen Gaussian. TEGA I is the cheapest to use, however, the first terms are qualitatively wrong while those of TEGA III are reasonable. Given the similarity between TEGA II and TEGA III we do not provide the TEGA II results in this figure.

Thus far we have only considered the convergence of different Gaussian based series representations of the matrix elements of the Boltzmann operator. It is of interest to check whether the usage of such a series representation is at all competitive with the more standard path-integral techniques. For this purpose we computed also the antidiagonal matrix elements using the discretized path-integral formula

$$\langle x|\exp(-\beta\hat{H})|-x\rangle = \int_{-\infty}^{\infty}\prod_{j=1}^{N} dx_j \langle x|\exp\left(-\frac{\beta\hat{H}}{N+1}\right) \times |x_1\rangle\cdot\langle x_1|\exp\left(-\frac{\beta\hat{H}}{N+1}\right) \times |x_2\rangle\cdots\langle x_N|\exp\left(-\frac{\beta\hat{H}}{N+1}\right)|-x\rangle, \tag{2.20}$$

where the matrix elements $\langle x_1|\exp(-\frac{\beta\hat{H}}{N+1})|x_2\rangle$, etc. were estimated using the TEGA I approximation Eq. (2.1) which is exact when the imaginary time is sufficiently small.

The results are shown in Fig. 6 for the antisymmetric matrix element, with $x_0=1$ and moderate ($\beta=0.3$) and low ($\beta=1$) temperature. One finds that in both cases, the number of time slices needed for the path-integral estimate is much

larger than the number of integrations needed to converge when using any of the three TEGA series representations. This implies that the Gaussian based series representation could provide a much cheaper route to numerical evaluation of the Boltzmann operator.

## IV. DISCUSSION

We have analyzed the convergence properties of three different thawed Gaussian series representations for the imaginary time propagator. TEGA I used the simplest Gaussian approximation, without symmetrization. TEGA II and TEGA III used a symmetrized Gaussian approximation for the zeroth-order term. The perturbation series is symmetrized term by term when using TEGA II, but it is not symmetrized when using TEGA III. When considering only the partition function, we find that the frozen Gaussian approximation is as accurate as the thawed Gaussian. Since it is cheaper to implement, it is the preferred route. However, when considering quantities which are sensitive to tunneling, we find that (a) the thawed Gaussian approximations are more accurate and the respective series converges to the numerically exact answer with significantly less iterations. (b) Within the thawed Gaussian class of approximations, the fully unsymmetrized form converges to the numerically exact answer with fewer configuration integrations than TEGA II and TEGA III. This implies that when one needs accurate answers, one should employ the unsymmetrized series representation. However, if one only needs a qualitative estimate, then the symmetrized form is more reliable. Finally, we find that the unsymmetrized series representation, based on the symmetrized form, is more efficient for use than the fully symmetrized series representation.

When comparing the thawed Gaussian forms with the frozen Gaussian, one should keep in mind that we compared with the optimized frozen Gaussian form. That is, the frozen Gaussian approximation depends sensitively on the initial choice of the width matrix. The optimal choice was found in Ref. [22] by minimizing the first-order correction to the partition function. It was this choice which then served as the basis for comparison with the thawed Gaussian in the present study. In contrast, the thawed Gaussian does not have this additional freedom; as the initial choice of the width matrix is determined by the condition that initially, the propagator reduces to the identity operator. This is an additional computational advantage of the thawed Gaussian approach. Conversely, the thawed Gaussian approach calls for the solution of $N^2$ coupled equations of motion for the width matrix. However, in systems with many degrees of freedom, it is the size of the Monte Carlo sample needed for convergence which is the typical bottleneck rather than the number of equations which need to be solved. It may therefore be that for "large" systems, the thawed Gaussian is the preferred route due to the smaller number of configuration integrations needed to converge the series.

It is remarkable that with the thawed Gaussians, less than five iterations are needed to converge matrix elements which are of the order of $10^{-26}$. This was achieved only by using quartic precision arithmetic. This rapid convergence suggests that this methodology can be very useful even for systems with many degrees of freedom. This conclusion is especially strengthened when comparing to the slow convergence we found for the antisymmetric matrix element based on a discretized path-integral representation. The Gaussian series based representation demands much less coordinate integrations then the discretized path integral, especially at low temperatures.

We gratefully acknowledge support of this work by a grant of the Israel Science Foundation. We also thank an anonymous referee for suggesting the comparison with a discretized path-integral estimate.

[1] B. J. Berne and D. Thirumalai, Annu. Rev. Phys. Chem. **37**, 401 (1986).
[2] N. Makri, Annu. Rev. Phys. Chem. **50**, 167 (1999).
[3] D. M. Ceperley, AIP Conf. Proc. **690**, 85 (2003).
[4] R. Giachetti and V. Tognetti, Phys. Rev. Lett. **55**, 912 (1985); Phys. Rev. B **33**, 7647 (1986).
[5] D. Thirumalai, R. W. Hall, and B. J. Berne, J. Chem. Phys. **81**, 2523 (1984).
[6] L. M. SéSé, Mol. Phys. **97**, 881 (1999).
[7] H. Kleinert, *Path Integrals in Quantum Mechanics, Statistics, Polymer Physics, and Financial Markets*, 3rd ed. (World Scientific, Singapore, 2004), Chap. 5.
[8] E. J. Heller, J. Chem. Phys. **75**, 2923 (1981).
[9] E. J. Heller, J. Chem. Phys. **62**, 1544 (1975).
[10] B. Hellsing, A. Nitzan, and H. Metiu, Chem. Phys. Lett. **123**, 523 (1986).
[11] P. A. Frantsuzov, A. Neumaier, and V. A. Mandelshtam, Chem. Phys. Lett. **381**, 117 (2003).
[12] P. A. Frantsuzov and V. A. Mandelshtam, J. Chem. Phys. **121**, 9247 (2004).
[13] P. A. Frantsuzov, D. Meluzzi, and V. A. Mandelshtam, Phys. Rev. Lett. **96**, 113401 (2006).
[14] V. A. Mandelshtam and P. A. Frantsuzov, J. Chem. Phys. **124**, 204511 (2006).
[15] P. A. Frantsuzov and V. A. Mandelshtam, J. Chem. Phys. **128**, 094304 (2008).
[16] J. Liu and W. H. Miller, J. Chem. Phys. **125**, 224104 (2006).
[17] W. H. Miller, Y. Zhao, M. Ceotto, and S. Yang, J. Chem. Phys. **119**, 1329 (2003).
[18] J. Shao and E. Pollak, J. Chem. Phys. **125**, 133502 (2006).
[19] E. Pollak and J. Shao, J. Phys. Chem. A **107**, 7112 (2003).
[20] S. Zhang and E. Pollak, Phys. Rev. Lett. **91**, 190201 (2003).
[21] J. Moix, E. Pollak, and J. Shao, Phys. Rev. A **80**, 052103 (2009).
[22] D. H. Zhang, J. Shao, and E. Pollak, J. Chem. Phys. **131**, 1 (2009).
[23] P. Hänggi, P. Talkner, and M. Borkovec, Rev. Mod. Phys. **62**, 251 (1990).